HHS Public Access

Author manuscript

Thromb Haemost. Author manuscript; available in PMC 2022 April 01.

Published in final edited form as:

Thromb Haemost. 2021 April ; 121(4): 506–517. doi:10.1055/s-0040-1719030.

Exome Sequencing Identifies Abnormalities in Glycosylation and *ANKRD36C* in Patients with Immune-Mediated Thrombotic Thrombocytopenic Purpura

Malay Kumar Basu[1], **Felipe Massicano**[1], **Lijia Yu**[1], **Konstantine Halkidis**[2], **Vikram Pillai**[3], **Wenjing Cao**[3], **Liang Zheng**[3], **X. Long Zheng**[3]

[1]Division of Genomic Diagnostics and Bioinformatics, Department of Pathology, The University of Alabama at Birmingham, Birmingham, Alabama, United States

[2]Division of Hematology/Oncology, Department of Medicine, The University of Alabama at Birmingham, Birmingham, Alabama, United States

[3]Department of Pathology & Laboratory Medicine, The University of Kansas Medical Center, Kansas City, Kansas, United States

Abstract

Background—Immune-mediated thrombotic thrombocytopenic purpura (iTTP) is a potentially fatal blood disorder, resulting from autoantibodies against ADAMTS13 (a disintegrin and metalloproteinase with a thrombospondin type 1 motif, member 13). However, the mechanism underlying anti-ADAMTS13 autoantibody formation is not known, nor it is known how genetic aberrations contribute to the pathogenesis of iTTP.

Methods—Here we performed whole exome sequencing (WES) of DNA samples from 40 adult patients with iTTP and 15 local healthy subjects with no history of iTTP and other hematological disorders.

Results—WES revealed variations in the genes involved in protein glycosylation, including O-linked glycosylation, to be a major pathway affected in patients with iTTP. Moreover, variations in the *ANKRD* gene family, particularly *ANKRD36C* and its paralogs, were also more prevalent in patients with iTTP than in the healthy controls. The ANKRD36 family of proteins have been implicated in inflammation. Mass spectrometry revealed a dramatic alternation in plasma glycoprotein profile in patients with iTTP compared with the healthy controls.

Address for correspondence Malay Kumar Basu, PhD, Division of Genomic Diagnostics and Bioinformatics, University of Alabama at Birmingham, Birmingham, AL 35249, United States, (malay@uab.edu). X. Long Zheng, MD, PhD, Department of Pathology & Laboratory Medicine, University of Kansas Medical Center, 5016 Delp, 3901 Rainbow Boulevard, Kansas City, KS 66160, United States, (xzheng2@kumc.edu; longzheng01@gmail.com).

Authors' Contributions

M.K.B. and X.L.Z. designed the research, performed the data analysis, and drafted the manuscript. F.M., L.Y., K.H., and W.C. performed the data collection and analysis. All authors contributed to the interpretation of the results and approved the final version of the manuscript.

Conflict of Interest

X.L.Z. is a speaker and a consultant for Alexion, Sanofi, and Takeda. X.L.Z. is also the cofounder of Clotsolution. All other authors declare no conflict of interest.

Conclusion—Altered glycosylation may affect the disease onset and progression in various ways: it may predispose patients to produce ADAMTS13 autoantibodies or affect their binding properties; it may also alter clearance kinetics of hemostatic and inflammatory proteins. Together, our findings provide novel insights into plausible mechanisms underlying the pathogenesis of iTTP.

Keywords

thrombotic thrombocytopenic purpura; glycosylation; mutations; pathogenesis; autoimmune diseases

Introduction

Immune-mediated thrombotic thrombocytopenic purpura (iTTP) is characterized by severe thrombocytopenia and hemolytic anemia with the fragmentation of red blood cells and/or signs and symptoms of organ dysfunction.[1,2] It is primarily caused by autoantibodies against a plasma metalloprotease, ADAMTS13 (a disintegrin and metalloproteinase with a thrombospondin type 1 motif, member 13). These autoantibodies bind and neutralize plasma ADAMTS13 activity.[3] ADAMTS13 is mainly synthesized in hepatic stellate cells and endothelial cells, which is released into the blood stream where it cleaves endothelial ultra-large von Willebrand factor (ULVWF) multimers.[4] Such a proteolytic cleavage is essential for maintaining the balance of delicate hemostasis. Severe deficiency of plasma ADAMTS13 activity results in an accumulation of ULVWF multimers on the activated endothelial surface, at the site of vascular injury where thrombi are formed, and in the circulating blood. These ULVWF multimers are hyperactive and able to recruit platelets from circulation,[5,6] leading to an enhanced rate of thrombus formation even at sites where no obvious vascular injury occurs.

To date, the risk factors and mechanisms underlying autoantibody formation in patients with iTTP are largely unknown. Previous studies have demonstrated that women of child-bearing age,[7] African origin,[8] with infections, and under certain medications, as well as genetic (e.g., human leukocyte antigen) background[9] are all associated with the development of iTTP. Nearly all ADAMTS13 autoantibodies are immunoglobulin Gs (IgGs) in nature, which appear to bind various parts of ADAMTS13, particularly the spacer domain to mediate its inhibitory function.[3] The role of the anti-ADAMTS13 IgG that binds to other parts of ADAMTS13 is not fully understood. A recent study has suggested that some antibodies that bind to the distal domain of ADAMTS13 may be able to stimulate ADAMTS13 activity through their effects on the conformations of ADATMS13.[10] ADAMTS13 and its only known substrate von Willebrand factor (VWF) are heavily glycosylated with both N-linked and O-linked oligosaccharides attached. Studies have also demonstrated that glycosylation patterns in both ADAMTS13[11] and VWF[12,13] may affect their interactions and subsequent proteolysis. Additionally, the aberrant glycosylation patterns in other soluble and cellular proteins may generate an aberrant immune response, which may result in autoantibody formation. This has been shown to be the case in many other autoimmune diseases.[14]

While severe deficiency of plasma ADAMTS13 activity is necessary, this alone is often not sufficient to cause an acute episode of TTP. This is exemplified by patients with inherited severe deficiency of plasma ADAMTS13 who did not develop acute TTP until later in life.[15] Infections or pregnancy are two of the most common environmental factors that trigger acute TTP in those with severe ADATMS13 deficiency.[16,17] Infections lead to the release of bacterial toxins, the action of neutrophils and their release of azurophilic granular contents such as human neutrophil peptide and histone/DNA complexes. All of these are shown to stimulate endothelial cells to release ULVWF[18,19] or activate complement factors.[20]

To identify novel candidate mutations that might be involved in autoimmunity and development of iTTP, we employed whole exome sequencing to determine the contribution of genetic variations in patients with acute iTTP. Our results indicate that variations in protein glycosylation appear to be a major associative factor in iTTP. We also establish an association between the variations in the *ANKRD36* family and iTTP; however, the function of the *ANKRD36* gene family of proteins remains largely unknown.

Methods

Patient Cohort

The institutional review board of the University of Alabama at Birmingham and the University of Kansas Medical Center approved the study protocol. Informed consent was obtained from each research participant. Forty patients with confirmed diagnosis of iTTP and 15 local matched healthy controls were included in the study. The inclusion criteria for iTTP[1,21] were (1) a patient with acute onset of severe thrombocytopenia (platelet count < 20 × 10^9/L) and microangiopathic hemolytic anemia (e.g., low hemoglobin, low haptoglobin, high Lactate dehydrogenase [LDH] and schistocytes on the peripheral blood smear, etc.) without other known causes and (2) plasma ADAMTS13 activity <10 U/dL (or <10% of normal) with detectable inhibitors (>0.4 U/mL) or elevated anti-ADAMTS13-IgG (>15 U/mL). All healthy control subjects were recruited from the local population who did not have a history of iTTP or any other hematological disorders and were matched for age and ethnic background with the iTTP subjects.

Sample Preparation

Genomic DNA was isolated from peripheral blood samples from iTTP patients and matched controls. The quality of genomic DNA (gDNA) was checked with the Agilent DNA/RNA analysis platform. The exome capture was performed using Roche SeqCap EZ Human Exome Kit v3.0 and sequenced on the Illumina Hiseq3000 platform.

Alignment and Variant Detection

The quality of the reads was checked with FastQC (v0.11.5) (http://www.bioinformatics.babraham.ac.uk/projects/fastqc). Raw reads were cleaned and trimmed using Trimmomatic (v0.36) keeping the quality scores larger than 20. The filtered and cleaned reads were mapped to UCSC hg19 reference using the BWA[22] (v0.7.10-r789) software with the BWA-MEM algorithm. After the alignment, the variants were called on the BAM files using the Genome Analysis Toolkit (GATK), following GATK best practices

recommendation (https://software.broadinstitute.org/gatk/best-practices/). Briefly, the steps were as follows: (1) markingduplicate reads using Picard (v2.8.3) MarkDuplicates; (2) local realignment using GATK (v3.7.0) RealignerTargetCreator and IndelRealigner; (3) recalibrate base using GATK BaseRecalibrator; (4) generate genomic variant call format (GVCF) files using GATK HaplotypeCaller with a minimum base quality requirement of 30. The generated GVCF files were then used to call joint genotypes for all the 55 samples in the cohort using the GATK GenotypeGVCFs tool. The resulting variant call format (VCF) files were then subjected to GATK Variant Quality Score Recalibration (VQSR) to filter variants, using HapMap[23] and 1000 Genomes Project data. The resulting file was annotated using ANNOVAR with the Combined Annotation Dependent Depletion (CADD) score, Clinvar, dnNSFP, 1000 Genomes allele frequencies, and snp138 data. All variants with 1000 Genomes allele frequency >0.05 were removed from the datasets to keep only the rare variants for further analysis. We also imposed one additional criterion for variant filtering keeping only those variants that are supported by ≥10 reads (read depth [DP] in VCF file ≥10).

Case–Control Association

A case–control association study was performed using the PLINK software (v. 1.9). To generate the input files for PLINK, VCF files were first filtered keeping only the nonsynonymous, stop-gain, and stop-loss variants. An in-house script was used to split all biallelic and multiallelic sites to monoallelic sites. Any position with absent genotypes was removed from the analysis. The files were then used as input files directly for PLINK and association studies were performed using Fisher's exact test as implemented in PLINK. Two sets of analyses were performed using PLINK with or without sex as a covariate. The multiple test correction was performed using the "q-value" package in R.

Gene-Based Association Analysis Using SKAT

Gene-based association with the disease was estimated using the SNP-set Kernel Association Test (SKAT) R package. For this, each single nucleotide variant (SNV) was coalesced within the boundary of the enclosing genes and the importance of each gene was tested for rare variants. The SKAT R-package uses an efficient resampling method to include extremely rare variants in the analysis. The SKAT null model was adjusted for small size and the CADD score for each variant was used as custom weights. Next, the weighted data were used for Burden, SKAT, and SKAT-O analysis with the "SKATBinary.SSD.All" function of the SKAT package.

Genotype with Disease Association

For finding the association of genotypes with the disease, we performed a regression analysis of the principal component of the genotype data with the clinical features. For this, we extracted all nonsynonymous and stop-gain/loss variants corresponding to all the significant genes found using the SKAT analysis above. We then created a "012" table using VCFTools.[24] The numbers 0, 1, and 2 represent unaffected, heterozygous, and homozygous variants, respectively. The table describes the state of each variant in each sample in our cohort. We then decomposed these data using the prcomp function in R. We extracted the

principal component 1 showing >70% of the variability in the data and estimated its linear regression with each of the quantitative clinical phenotypes mentioned in ►Table 1.

Epistasis Analysis

To identify any possible synergistic effect of mutations, we performed an epistatic analysis using only nonsynonymous mutations that pass our filtering criteria. We used PLINK (ver. 1.9) to carry out the epistasis among these variants. The pairwise interacting variants were then assigned their corresponding gene names. For each gene pair, only the lowest *p*-values were kept for the analysis. We then constructed an undirected network of interacting genes with –log10 converted *p*-values as weights using Cytoscape.[25] In this network, the nodes represent the genes, edges are epistatic relationships, and the edge weight is determined by the *p*-values. We identified hub genes in the network using the cytoHubba[26] app using three measures of centrality: node degree, edge percolated component (EPC), and betweenness.

Plasma Glycoproteome in iTTP Patients and Controls

Glycoproteins in patient and control plasmas (30μL each) were enriched with a Pierce glycoprotein purification ConA kit (Thermo Fisher Scientific) following manufacturer's instructions. The eluates were quantified, and 20 μg per subpool were then diluted in NuPAGE LDS sample buffer, reduced with DTT, and denatured at 70°C for 10 minutes. Samples were separated halfway onto a NuPAGE 10% Bis-Tris Protein gel. The gel was then stained for visualization and each sample lane was excised into three molecular-weight fractions, and each fraction was then digested with Trypsin Gold. Peptides extracted from each fraction were then reconstituted in 0.1% formic acid/ddH_2O at approximately 0.2 μg/μL. The peptides were estimated using a SCIEX 5600 TripleTOF mass spectrometer at the UAB Proteomics Core facility.

Differential Glycoprotein Estimation

Spectral counts of the glycoproteins estimated with mass spectrometry were normalized after removing all genes whose counts were 0 in more than 50% of the samples. The normalized count data were used for the hierarchical clustering of the samples using R package *pheatmap*.[27] For the detection of the outliers, we cut the tree at level 1 to generate two clusters. The largest cluster with a common root was used for all further analyses. For differential expression, we used the R Bioconductor package msmsTests.[28] Cases and control groups were compared using a negative binomial model, as implemented in the *msms.edgeR* function in the package. The *p*-values obtained from the analysis were adjusted for multiple test correction using Benjamini–Hochberg false discovery rate (FDR) calculation.

Gene-Set Enrichment Analysis

We used either the R package clusterProfiler[29] or FGSEA[30] for gene-set enrichment analysis (GSEA) either using gene ontology[31] or REACTOME[32] databases.

Results

Patient Characteristics

Summary of demographic, clinical, and laboratory information of 40 iTTP patients are shown in ►Table 1. Of these, 14 were males (35%) and 26 were females (65%) with a median age of 44. The median acute TTP episode in these patients was 1.0. On admission, the median platelet count and hematocrit were 13.0×10^9/L and 24.0%, respectively. The median serum level of LDH was 861.5 U/L and that of creatine was 1.3 mg/dL. All patients had serum haptoglobin <30 - mg/dL and plasma ADAMTS13 activity <5 U/dL (or <5%). The median ADAMTS13 inhibitor was 1.2 U/mL. Therapeutic plasma exchange (TPE) was performed in all patients with the median number of procedures of 15 per patient. Corticosteroids were prescribed to 92.5% of patients. Only one-third of patients received rituximab for therapy. Remission, exacerbation, relapse, and death occurred in 40, 22.5, 27.5, and 5%, respectively, in this cohort of patients (►Table 1).

Sequencing and Variant Detection

The overall workflow of the exome sequence data analysis is shown as a flowchart in ►Fig. 1. We performed exome sequencing of the gDNA samples obtained from 40 iTTP patients and15 healthy controls using the Illumina HiSeq3000 platform. On average, we received 64 million paired-end reads per sample. When aligning the reads against the human reference hg19 genome using the BWA-MEM algorithm,[22] approximately 76% of the reads were mapped to the target genome at the mapping quality score>20. The variants in each sample were identified using GATK. On average, approximately 13,000 nonsynonymous and approximately 14,000 synonymous variants were obtained for each file.

In most of our analyses, we focused on only the nonsynonymous mutations. First, we filtered out all the SNVs where the minor allele frequency is >0.05 in the 1000 Genomes Project reported by ANNOVAR.[33] This is assuming that disease variants will be rare in the general population. Then, we kept only nonsynonymous coding variants with two additional types of variants as reported by ANNOVAR: “stop gain” and “stop loss.” All variants were filtered with DP ≥10 (i.e., each variant is supported byat least 10 reads). We also subjected the VCF files through the GATK variant filtering method, VQSR. For some analyses, we only used the VQSR “PASS” filter. On average approximately 80% nonsynonymous and approximately 88% synonymous mutations passed the VQSR “PASS” filter. We could not detect any batch effect in the samples by clustering the samples based on the mutation profile.

Involvement of the ANKRD36 Family in iTTP

To identify potential genetic abnormalities that may contribute to the pathogenesis of iTTP, we performed a case–control association study. Looking at only the exonic rare SNVs with alternate allele frequency less than 5% in the 1000 Genomes Project and those passing our filtering criteria, there were 22,158 nonsynonymous variants, 20,159 synonymous variants, 227 stop gain, 21 stop loss, and 431 variants of unknown type. Inspecting the frequency of these variants in iTTP samples, we found that none of these variants was present universally in all the samples. The most common variants were present at most 37.5% of the samples,

consistent with the presumption that iTTP is a multifactorial disorder, with no single variant could be considered causative, and these variants might provide the genetic background necessary for the progression of iTTP caused by acquired severe deficiency of plasma ADAMTS13 activity.

Using the software PLINK and Fisher's exact test, we identified SNVs that were statistically associated with iTTP patients compared with the controls. We found 455 SNVs with a *p*-value of less than 0.05 in the PLINK results. However, none of them could achieve significance after FDR correction (►Supplementary TableS1, available in the online version), suggesting that a larger and balanced (cases vs. controls) sample size may be required to achieve genome level significance. A power analysis using the software PAGEANT[34] and the effect size calculated from the best performing alleles of ANKRD36C showed the required sample number to be approximately 1,500 to achieve genome-wide statistical significance.

Regardless of the FDR, we identified the alleles with the lowest *p*-values belonging to the following genes: *ANKRD36C, MUC3A, CNNM1, MTCH2, KMT2C, MYO5B, RFPL2* and *3, RGPD3, NBPF10*, and *PRR23A* (►Fig. 2A). The top gene in this analysis was *ANKRD36C*, an ankyrin (ANK) domain-containing protein family in the human genome (►Table 2). We validate ANKRD36C involvement in iTTP using other methods (see below). A repeat analysis using sex as a covariate gave similar results with alleles of *ANKRD36C* having the lowest *p*-values (►Supplementary Fig. S1, available in the online version). Except at chr2: 96592982, all the variants are present in the dbSNP database.[35] Seven out of 10 variants are only present in iTTP patients (►Table 2).

ANKRD36C is one of the three paralogs of ANKDRD36 family containing AKDRD36A, AKDRD36B, and AKDRD36C. All these genes are located on chromosome 2 in the human genome, and their functions are unknown. These genes are characterized by ANK domains primarily involved in protein–protein interactions. To gain insight into the possible function of the ANKRD36 family, we looked at the expressions of ANKRD36A–C in the Genotype-Tissue Expression (GTEx) database.[36] ANKRD36A and ANKRD36B have very similar expression patterns with the highest expression seen in the testes and brain (►Supplementary Fig. S2, available in the online version). ANKRD36C also has a very similar expression pattern, except its highest expression is found in salivary glands (►Supplementary Fig. S2, available in the online version). Thus, it is reasonable to assume that these genes may have complementary roles, and the whole family might be involved in the pathogenesis of iTTP.

Identification of Glycosylation As an Affected Pathway in iTTP

To identify pathways involved in iTTP, we searched the gene ontology database with the list of affected genes. The search immediately identified "immune response" to be the major affected pathway in iTTP patients (►Fig. 2B). We used R package clusterProfiler[29] for this analysis. This is not surprising, given that iTTP is an autoimmune disorder. However, more interestingly, we also identified the mutations in the genes involved in protein glycosylation, including the C-type lectin receptor signaling pathway and O-linked glycosylation or glycan processing in these patients (►Fig. 2B). A small number of patients also had mutations in

the gene involved in cobalamin metabolic processing and the RIG-I signaling pathway (►Fig. 2B). As an alternative, we also performed GSEA of the affected gene sets using a sorted list of p-values from association analysis and REACTOME[32] database (►Supplementary Table S2 and ►Supplementary Fig. S3, available in the online version). The result again identified O-glycosylation as an affected pathway thus bolstering our hypothesis that O-glycosylation plays a major role in the pathogenesis of iTTP (►Supplementary Fig. S3, available in the online version).

Gene-Based Kernel Association Analysis

To verify the involvement of ANKRD36C and MUCIN as revealed by the PLINK association analysis and to overcome lower statistical power of association analysis using a small sample size, we performed a gene-based association analysis using SKAT as implemented in R software package SKAT. The method combines a burden test with an association test to evaluate each gene, given a specific trait. We used only nonsynonymous, stop-gain, and stop-loss data in the analysis, using SKATBinary.SSD.All function as provided by the SKAT package (see the Methods section). To make the analysis more meaningful, we used the CADD score for each variant as custom weights (►Fig. 3 and ►Supplementary Table S3, available in the online version). There are 100 genes for which minimum achievable *p*-values were too small for calculation ("MAP" = 1; ►Supplementary Table S3, available in the online version). By considering only the raw *p*-values, the lowest *p*-values (10^{-6}) were seen for the genes ANKRD36C and TAS2R19. However, the burden test must consider the abundance of the variant alleles for a particular gene in cases versus control as an indication of whether the gene is disease-associated. With a *p*-value cutoff 0.05 and sorted based on the total number of variant alleles in cases, we found MUCIN genes dominated the most significant positions, but more importantly, ANKRD36C also had the lowest *p*-value in the top three positions on the list (►Fig. 3 and ►Supplementary Table S3, available in the online version). These results support our hypothesis that ANKRD36C may play a very important role in the pathogenesis of iTTP.

Association of Variants with Clinical Features

As apparent from the previous sections, iTTP is not a single-gene disorder, but many genes participate in creating a genetic milieu favorable for the disease progression. To find how the overall mutational environment affects the disease phenotype, we decided to determine the statistical association of variants in the genome and a set of clinical features is shown in ►Table 1. The overall genetic landscape can be represented by the first principal component of the sample versus variant matrix (see the Methods section). We created this matrix by selecting all the nonsynonymous and stop-gain/loss variants corresponding to all the genes identified using SKAT analysis above and then decoding their presence in each sample with values 0, 1, and 2, corresponding to no variants, heterozygous, and homozygous alleles, respectively (see the Methods section). The first principal component of this matrix was then regressed linearly on quantitative numerical clinical features (►Supplementary Table S4, available in the online version). We found three clinical features to have mild but statistically significant association: ADAMTS13 antibody level ($R^2 = 0.131$, $p = 0.025$), haptoglobin level ($R^2 = 0.129$, $p = 0.036$), and creatine ($R^2 = 0.129$, $p = 0.036$). The fact that the

ADAMTS13 antibody has the highest regression value validated our belief that the mutational landscape of the patient genome truly contributes to the disease phenotype.

Epistatic Network Analysis

An epistatic analysis identifies the interaction between alleles. With the possibility in mind that iTTP is probably a multifactorial disorder, we performed an epistatic analysis of the alleles to identify any possible synergistic effect between pairs of alleles. For this, only nonsynonymous mutations that pass our filtering criteria were used (see the Methods section). We used PLINK to carry out the epistasis among these variants. The pairwise-interacting variants were then assigned their corresponding gene names. For each gene pair, only the lowest *p*-values were kept for the analysis. We then constructed a network of interacting genes with –log10 converted *p*-values as weights using Cytoscape.

The resulting network had 3,559 nodes with a clustering coefficient of 0.037. We identified hub genes in this network using the cytoHubba app in Cytoscape[25] (►Fig. 4A). Interestingly, the top gene in two measures of centrality—node degree and EPC—is *ANKRD36C*. For the other measures of centrality, betweenness, the genes are tied in the first rank with phosphodiesterase 4D (PDE4D)-interacting protein (PDE4DIP[37]; ►Supplementary Table S5, available in the online version). A partial subnetwork of the top two genes (**ANKRD36** and **PDE4DIP**) of this network is shown in ►Fig. 4A. PDE4DIP is a gene involved in microtubule dynamics.[38] The defects in this gene have been implicated in myeloproliferative disorder associated with eosinophilia, as well as in pineoblastoma.[39] The role of this gene in iTTP remains to be investigated. An analysis of the sorted gene list by EPC with GSEA again confirms the involvement of O-linked glycosylation (►Fig. 4B and ►Supplementary Table S6, available in the online version).

iTTP Patients and Control Samples Differ in Glycoprotein Profile

To prove experimentally whether glycosylation defect is a causative factor in iTTP, we compared glycoproteins in 15 iTTP versus 15 control samples using mass spectrometry (see the Methods section). After filtering out genes with low expression (count 0 in >50% of samples), we detected altogether 204 proteins in these samples. We detected seven samples as outliers (see the Methods section and ►Supplementary Fig. S4, available in the online version). A hierarchical clustering of the samples based on normalized spectral counts immediately supported our earlier findings that the glycoprotein repertoire is drastically different between cases and controls (►Fig. 5A). Except for one TTP sample, iTTP and normal samples formed distinct clusters. The outlier TTP patient had unusually long hospital stay (168 days, compared with the median value of 19 days) and received very high TPE (117 compared with the median value of 15). Other than these, at this time, the reason for this patient clustering with control samples is unknown. To identify the glycoproteins that are differentially expressed in cases versus controls, we performed a differential analysis. For this, we used a negative binomial model (function *msms.edgeR*) as implemented in the R Bioconductor package *msmsTests*.[28] We could identify 42 proteins to be differentially expressed ($p < 0.05$), out of which 11proteins passed the FDR (< 0.05; ►Supplementary Table S7, available in the online version).

Out of these 42 proteins, 14 were found to be overexpressed in iTTP patients, and 28 were underexpressed (►Supplementary Table S7, available in the online version). An inspection of the gene list sorted based on log-fold change (►Supplementary Table S7, available in the online version) between iTTP and control (►Fig. 5B) immediately reveals candidates involved in immune reactions and coagulation activities. The top gene overexpressed in iTTP samples (log2-fold change >4) is S100A8, a gene involved in immune response and inflammatory processes.[40] The other important genes overexpressed in iTTP samples compared with control are APOE, IGHD, FCGBP, PRG4, and C4BPB. These genes are mostly involved in immune reactions.

Interestingly, three top genes repressed in iTTP samples are all HDL-associated. They are APOA4, haptoglobin, and haptoglobin-related protein. These genes are HDL-associated proteins and are involved in the innate immune response. HDL plays a crucial role in both innate and adaptive immunity and repression of HDL has already been reported in various autoimmune disorders.[41] HDL has also been shown to prevent VWF self-association.[42] Our data further support these earlier findings and establish the repression of HDL being associated with iTTP. Besides these, a large number of complement factor and coagulation pathway genes are also differentially expressed in iTTP versus control samples. Overall, the results confirm our earlier prediction that a change in glycosylation may be involved in iTTP. These results also indicate an important role of lipid metabolism in the pathogenesis of iTTP.

Discussion

In the present study, we demonstrate that while there is not any single gene mutation identified to be a causative factor for iTTP, mutations in genes related to protein glycosylation, particularly the O-linked glycosylation, and the *ANKRD36* family, particularly the *ANKR36C*, show the strongest statistical association with iTTP patients compared with healthy controls. Further studies are needed to dissect the exact roles that this gene family plays in the pathogenesis of iTTP.

Defects in glycosylation are known to be involved in various autoimmune disorders, including rheumatoid arthritis (RA), systemic lupus erythematosus (SLE), autoimmune hemolytic anemia, IgA nephropathy, and Graves' disease.[43] In patients with RA, serum levels of agalactosyl IgG predict the outcome of early synovitis.[44] Mice with increased agalactosyl IgG develop spontaneous arthritis,[45] suggesting that altered glycosylation of IgGs may change the antibody effector function. Similar findings are reported for SLE.[46] In IgA nephropathy, there are abnormalities in O-linked, but not in N-linked glycosylation on IgA molecules.[47] The reduced level of galactose on the O-linked oligosaccharides in the hinge region may result from a B-cell-specific decrease of β1,3-GalTase enzyme activity.[48] The defective glycosylation may result in IgA aggregation,[49] the formation of IgG/IgA1 immune complexes, and IgA nephropathy.[50]

iTTP is yet another autoimmune disorder, resulting from autoantibodies against ADAMTS13 that bind and inhibit plasma ADAMTS13 activity.[3] Most of the inhibitory antibodies bind the nonlinear or conformational epitopes in the spacer domain of

ADAMTS13 for inhibition.[3] Chui et al demonstrate that mutation of a single gene, encoding α-mannosidase II, which regulates the complex branching pattern of extracellular asparagine N-linked oligosaccharide chains, results in a systemic autoimmune disease similar to human SLE,[46] suggesting the genetic cause of autoimmune disease provoked by a defect in the pathway of protein N-glycosylation. It remains speculative at this point whether or how abnormalities in protein glycosylation would affect the pathology of iTTP (►Fig. 6). The altered glycosylation may affect the formation of anti-ADAMTS13 autoantibodies, binding epitopes or affinities, and functionalities of these immune complexes. Additional animal studies are needed to address these fundamental questions. The observed glycosylation defect might also be the result of the disease state rather than a causative factor. Regardless, our results for the first time show that glycosylation defect is involved in iTTP. The actual nature of this involvement remains to be investigated.

The ANKRD36 family of proteins contain at least one ANK repeat domain repeat, a conserved domain of approximately 33 amino acids, which was originally identified in ANK. ANK repeat has been described as an L-shaped structure consisting of a β-hairpin and two α-helices as in BCL-3,[51] and mostly mediates protein–protein interaction. The functions of the *ANKRD36* family are essentially unknown. ANKRD36 may be related to inflammation as plasma levels of circulating *ANKRD36* RNA are dramatically elevated in patients with type 2 diabetes mellites[52]; silencing *ANKRD36* RNA in cultured rat embryonic ventricular cardiomyocytes results in an antiapoptotic and anti-inflammatory effect stimulated by lipopolysaccharides.[53] Mutations in *ANKRD26*, the closest homolog of *ANKRD36*, are associated with hereditary thrombocytopenia[54] and myeloid malignancies.[55] Another ANK domain protein, ANKRD55, is a known gene associated with many autoimmune diseases, like multiple sclerosis and RA.[56] Further investigation into the biological functions of the *ANRDK26/36* family in animal models, particularly in the setting of ADAMTS13 deficiency, may shed new light on pathogenic mechanisms of iTTP and other hematological or inflammatory disorders (►Fig. 6).

Overall, we believe that autoimmunity of iTTP is a result of cross-reactive antibodies against key iTTP molecules, such as ADAMTS13, presumably in response to external pathogenic agents, such as a bacterial infection. The cross-reactivity is brought about by the genetic propensity of the altered glycosylation pattern (►Fig. 6).

Supplementary Material

Refer to Web version on PubMed Central for supplementary material.

Funding

This study was supported by National Heart, Lung, and Blood Institute (HL115187 and HL144552–01A1).

References

1. Saha M, McDaniel JK, Zheng XL. Thrombotic thrombocytopenic purpura: pathogenesis, diagnosis and potential novel therapeutics. J Thromb Haemost 2017;15(10):1889–1900 [PubMed: 28662310]

2. Rock GA, Shumak KH, Buskard NA, et al.; Canadian Apheresis Study Group. Comparison of plasma exchange with plasma infusion in the treatment of thrombotic thrombocytopenic purpura. N Engl J Med 1991;325(06):393–397 [PubMed: 2062330]

3. Casina VC, Hu W, Mao JH, et al. High-resolution epitope mapping by HX MS reveals the pathogenic mechanism and a possible therapy for autoimmune TTP syndrome. Proc Natl Acad Sci U S A 2015;112(31):9620–9625 [PubMed: 26203127]

4. Dong JF, Moake JL, Nolasco L, et al. ADAMTS-13 rapidly cleaves newly secreted ultralarge von Willebrand factor multimers on the endothelial surface under flowing conditions. Blood 2002;100 (12):4033–4039 [PubMed: 12393397]

5. Chauhan AK, Motto DG, Lamb CB, et al. Systemic antithrombotic effects of ADAMTS13. J Exp Med 2006;203(03):767–776 [PubMed: 16533881]

6. Banno F, Chauhan AK, Kokame K, et al. The distal carboxylterminal domains of ADAMTS13 are required for regulation of in vivo thrombus formation. Blood 2009;113(21):5323–5329 [PubMed: 19109562]

7. Zheng XL, Kaufman RM, Goodnough LT, Sadler JE. Effect of plasma exchange on plasma ADAMTS13 metalloprotease activity, inhibitor level, and clinical outcome in patients with idiopathic and nonidiopathic thrombotic thrombocytopenic purpura. Blood 2004;103(11):4043–4049 [PubMed: 14982878]

8. Martino S, Jamme M, Deligny C, et al.; French Reference Center for Thrombotic Microangiopathies. Thrombotic thrombocytopenic purpura in black people: impact of ethnicity on survival and genetic risk factors. PLoS One 2016;11(07):e0156679

9. Coppo P, Busson M, Veyradier A, et al.; French Reference Centre For Thrombotic Microangiopathies. HLA-DRB111: a strong risk factor for acquired severe ADAMTS13 deficiency-related idiopathic thrombotic thrombocytopenic purpura in Caucasians. J Thromb Haemost 2010;8(04):856–859 [PubMed: 20141578]

10. South K, Luken BM, Crawley JT, et al. Conformational activation of ADAMTS13. Proc Natl Acad Sci U S A 2014;111(52):18578–18583 [PubMed: 25512499]

11. Nowak AA, O'Brien HER, Henne P, et al. ADAMTS-13 glycans and conformation-dependent activity. J Thromb Haemost 2017;15 (06):1155–1166 [PubMed: 28370891]

12. McGrath RT, van den Biggelaar M, Byrne B, et al. Altered glycosylation of platelet-derived von Willebrand factor confers resistance to ADAMTS13 proteolysis. Blood 2013;122(25):4107–4110 [PubMed: 24106205]

13. McKinnon TA, Chion AC, Millington AJ, Lane DA, Laffan MA. N-linked glycosylation of VWF modulates its interaction with ADAMTS13. Blood 2008;111(06):3042–3049 [PubMed: 17975018]

14. Li X, Xu J, Li M, et al. Aberrant glycosylation in autoimmune disease. Clin Exp Rheumatol 2020;38(04):767–775 [PubMed: 31694739]

15. van Dorland HA, Taleghani MM, Sakai K, et al.; Hereditary TTP Registry. The International Hereditary Thrombotic Thrombocytopenic Purpura Registry: key findings at enrollment until 2017. Haematologica 2019;104(10):2107–2115 [PubMed: 30792199]

16. Fujimura Y, Kokame K, Yagi H, et al. Hereditary deficiency of ADAMTS13 activity: Upshaw–Schulman syndrome. In: Rodgers G, ed. ADAMTS13 Biology and Disease. Cham: Springer; 2015:73–90

17. Furlan M, Lämmle B. Deficiency of von Willebrand factor-cleaving protease in familial and acquired thrombotic thrombocytopenic purpura. Baillieres Clin Haematol 1998;11(02):509–514 [PubMed: 10097823]

18. Michels A, Albánez S, Mewburn J, et al. Histones link inflammation and thrombosis through the induction of Weibel-Paladebody exocytosis. J Thromb Haemost 2016;14(11):2274–2286 [PubMed: 27589692]

19. Liu F, Huang J, Sadler JE. Shiga toxin (Stx)1B and Stx2B induce von Willebrand factor secretion from human umbilical vein endothelial cells through different signaling pathways. Blood 2011;118 (12):3392–3398 [PubMed: 21816831]

20. Johansson PI, Windeløv NA, Rasmussen LS, Sørensen AM, Ostrowski SR. Blood levels of histone-complexed DNA fragments are associated with coagulopathy, inflammation and

endothelial damage early after trauma. J Emerg Trauma Shock 2013;6(03):171–175 [PubMed: 23960372]

21. Scully M, Cataland S, Coppo P, et al.; International Working Group for Thrombotic Thrombocytopenic Purpura. Consensus on the standardization of terminology in thrombotic thrombocytopenic purpura and related thrombotic microangiopathies. J Thromb Haemost 2017;15(02):312–322 [PubMed: 27868334]
22. Li H, Durbin R. Fast and accurate long-read alignment with Burrows-Wheeler transform. Bioinformatics 2010;26(05):589–595 [PubMed: 20080505]
23. International HapMap C. The International HapMap Project. Nature 2003;426:789–796 [PubMed: 14685227]
24. Danecek P, Auton A, Abecasis G, et al.; 1000 Genomes Project Analysis Group. The variant call format and VCFtools. Bioinformatics 2011;27(15):2156–2158 [PubMed: 21653522]
25. Shannon P, Markiel A, Ozier O, et al. Cytoscape: a software environment for integrated models of biomolecular interaction networks. Genome Res 2003;13(11):2498–2504 [PubMed: 14597658]
26. Chin CH, Chen SH, Wu HH, Ho CW, Ko MT, Lin CY. cytoHubba: identifying hub objects and sub-networks from complex interactome. BMC Syst Biol 2014;8(Suppl 4):S11 [PubMed: 25521941]
27. Kolde R. Pheatmap: pretty heatmaps. R package version 2012;1
28. Gregori J, Sanchez A, Villanueva J msmsTests: LC-MS/MS Differential Expression Tests. 2020
29. Yu G, Wang LG, Han Y, He QY. clusterProfiler: an R package for comparing biological themes among gene clusters. OMICS 2012; 16(05):284–287 [PubMed: 22455463]
30. Korotkevich G, Sukhov V, Sergushichev A. Fast gene set enrichment analysis. bioRxiv 2019. Doi: 10.1101/060012
31. Harris MA, Clark J, Ireland A, et al.; Gene Ontology Consortium. The Gene Ontology (GO) database and informatics resource. Nucleic Acids Res 2004;32(Database issue):D258–D261 [PubMed: 14681407]
32. Fabregat A, Jupe S, Matthews L, et al. The reactome pathway knowledgebase. Nucleic Acids Res 2018;46(D1):D649–D655 [PubMed: 29145629]
33. Wang K, Li M, Hakonarson H. ANNOVAR: functional annotation of genetic variants from high-throughput sequencing data. Nucleic Acids Res 2010;38(16):e164
34. Derkach A, Zhang H, Chatterjee N. Power Analysis for Genetic Association Test (PAGEANT) provides insights to challenges for rare variant association studies. Bioinformatics 2018;34(09):1506–1513 [PubMed: 29194474]
35. Sherry ST, Ward MH, Kholodov M, et al. dbSNP: the NCBI database of genetic variation. Nucleic Acids Res 2001;29(01):308–311 [PubMed: 11125122]
36. Battle A, Brown CD, Engelhardt BE, Montgomery SBGTEx Consortium Laboratory, Data Analysis &Coordinating Center (LDACC)—Analysis Working Group Statistical Methods groups—Analysis Working Group Enhancing GTEx (eGTEx) groups NIH Common Fund NIH/NCI NIH/NHGRI NIH/NIMH NIH/NIDA Biospecimen Collection Source Site—NDRI Biospecimen Collection Source Site—RPCI Biospecimen Core Resource—VARI Brain Bank Repository—University of Miami Brain Endowment Bank Leidos Biomedical—Project Management ELSI Study Genome Browser Data Integration &Visualization—EBI Genome Browser Data Integration &Visualization—UCSC Genomics Institute, University of California Santa Cruz Lead analysts Laboratory, Data Analysis &Coordinating Center (LDACC) NIH program management Biospecimen collection Pathology eQTL manuscript working group. Genetic effects on gene expression across human tissues. Nature 2017;550(7675):204–213 [PubMed: 29022597]
37. Shapshak P. Molecule of the month, PDE4DIP. Bioinformation 2012;8(16):740–741 [PubMed: 23055623]
38. Wang Z, Zhang C, Qi RZ. A newly identified myomegalin isoform functions in Golgi microtubule organization and ER-Golgi transport. J Cell Sci 2014;127(Pt 22):4904–4917 [PubMed: 25217626]
39. Snuderl M, Kannan K, Pfaff E, et al. Recurrent homozygous deletion of DROSHA and microduplication of PDE4DIP in pineoblastoma. Nat Commun 2018;9(01):2868 [PubMed: 30030436]

40. Wang S, Song R, Wang Z, Jing Z, Wang S, Ma J. S100A8/A9 in inflammation. Front Immunol 2018;9:1298 [PubMed: 29942307]
41. Kaji H. High-density lipoproteins and the immune system. J Lipids 2013;2013:684903
42. Chung DW, Chen J, Ling M, et al. High-density lipoprotein modulates thrombosis by preventing von Willebrand factor self-association and subsequent platelet adhesion. Blood 2016; 127(05):637–645 [PubMed: 26552698]
43. Delves PJ. The role of glycosylation in autoimmune disease. Autoimmunity 1998;27(04):239–253 [PubMed: 9623502]
44. Bodman-Smith K, Sumar N, Sinclair H, Roitt I, Isenberg D, Young A. Agalactosyl IgG [Gal(o)]– an analysis of its clinical utility in the long-term follow-up of patients with rheumatoid arthritis. Br J Rheumatol 1996;35(11):1063–1066 [PubMed: 8948290]
45. Jeddi PA, Bodman-Smith KB, Lund T, et al. Agalactosyl IgG and beta-1,4-galactosyltransferase gene expression in rheumatoid arthritis patients and in the arthritis-prone MRL lpr/lpr mouse. Immunology 1996;87(04):654–659 [PubMed: 8675223]
46. Chui D, Sellakumar G, Green R, et al. Genetic remodeling of protein glycosylation in vivo induces autoimmune disease. Proc Natl Acad Sci U S A 2001;98(03):1142–1147 [PubMed: 11158608]
47. Allen AC, Harper SJ, Feehally J. Galactosylation of N- and O-linked carbohydrate moieties of IgA1 and IgG in IgA nephropathy. Clin Exp Immunol 1995;100(03):470–474 [PubMed: 7774058]
48. Allen AC, Topham PS, Harper SJ, Feehally J. Leucocyte beta 1,3 galactosyltransferase activity in IgA nephropathy. Nephrol Dial Transplant 1997;12(04):701–706 [PubMed: 9140997]
49. Hiki Y, Iwase H, Kokubo T, et al. Association of asialo-galactosyl beta 1–3N-acetylgalactosamine on the hinge with a conformational instability of Jacalin-reactive immunoglobulin A1 in immunoglobulin A nephropathy. J Am Soc Nephrol 1996;7(06):955–960 [PubMed: 8793806]
50. Novak J, Julian BA, Tomana M, Mestecky J. IgA glycosylation and IgA immune complexes in the pathogenesis of IgA nephropathy. Semin Nephrol 2008;28(01):78–87 [PubMed: 18222349]
51. Collins PE, Grassia G, Colleran A, et al. Mapping the interaction of B cell leukemia 3 (BCL-3) and nuclear factor κB (NF-κB) p50 identifies a BCL-3-mimetic anti-inflammatory peptide. J Biol Chem 2015;290(25):15687–15696 [PubMed: 25922067]
52. Fang Y, Wang X, Li W, et al. Screening of circular RNA sand validation of circANKRD36 associated with inflammation in patients with type 2 diabetes mellitus. Int J Mol Med 2018;42(04):1865–1874 [PubMed: 30066828]
53. Wang Q, Tao S, Zhu N, Li T, Yu L. Silencing circular RNA circANKRD36 remits lipopolysaccharide-induced inflammatory damage by regulating microRNA-15/MyD88. J Cell Biochem 2020;121(03):2704–2712 [PubMed: 31692058]
54. Noris P, Perrotta S, Seri M, et al. Mutations in ANKRD26 are responsible for a frequent form of inherited thrombocytopenia: analysis of 78 patients from 21 families. Blood 2011;117(24): 6673–6680 [PubMed: 21467542]
55. Noris P, Favier R, Alessi MC, et al. ANKRD26-related thrombocytopenia and myeloid malignancies. Blood 2013;122(11):1987–1989 [PubMed: 24030261]
56. Ugidos N, Mena J, Baquero S, et al. Interactome of the autoimmune risk protein ANKRD55. Front Immunol 2019;10:2067 [PubMed: 31620119]
57. Ionita-Laza I, Lee S, Makarov V, Buxbaum JD, Lin X. Sequence kernel association tests for the combined effect of rare and common variants. Am J Hum Genet 2013;92(06):841–853 [PubMed: 23684009]

What is known about this topic?

- iTTP is a potentially fatal blood clotting disorder, resulting from autoantibodies against ADAMTS13.
- However, the mechanism underlying anti-ADAMTS13 autoantibody formation is not known, nor the genetic abnormalities contributing to the pathogenesis of iTTP.

What does this paper add?

- We performed whole exome sequencing (WES) of DNA samples from 40 adult patients with iTTP with 15 healthy subjects.
- WES revealed variations in the genes involved in protein glycosylation, including O-linked glycosylation, to be a major pathway affected in patients with iTTP.
- Moreover, variations in the *ANKRD* gene family, particularly ANKRD36C and its paralogs, were also more prevalent in patients with iTTP than in the healthy controls.
- Mass spectrometry revealed the dramatic alternation in the plasma glycoprotein profile in patients with iTTP compared with the healthy controls.
- We conclude that the alterations in glycosylation and ANKRD36 family proteins may predispose patients to the development of iTTP.

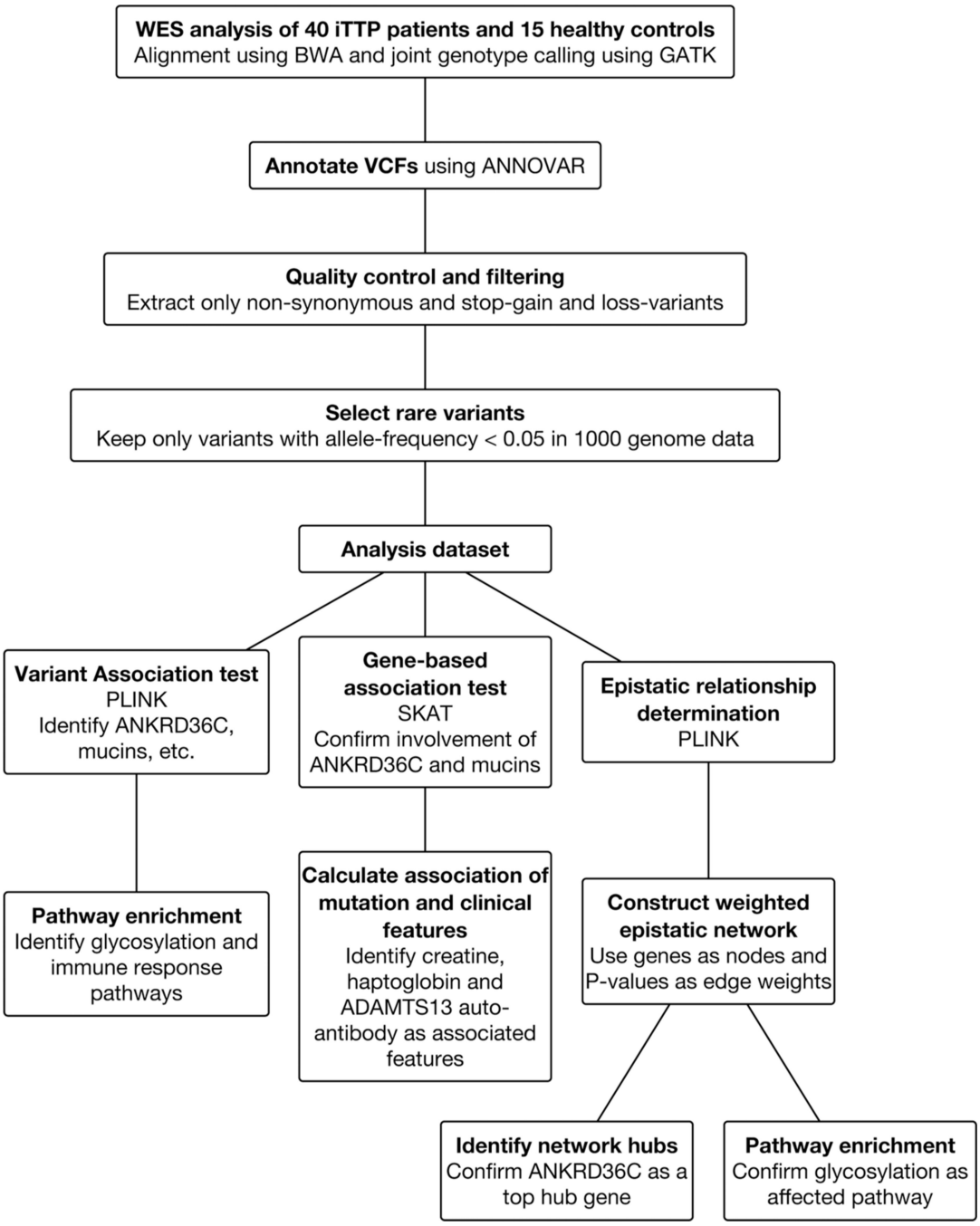

Fig. 1.

Flowchart depicting the process for identifying the abnormalities in glycosylation and ANKRD family members in iTTP. Here, whole exome sequencing (WES) was performed for 40 patients with iTTP and 15 local and ethnic healthy controls. Note that we provide evidence of the involvement of glycosylation pathways in iTTP, independently, using mass spectrometry data, which are not shown in this figure. iTTP, immune-mediated thrombotic thrombocytopenic purpura.

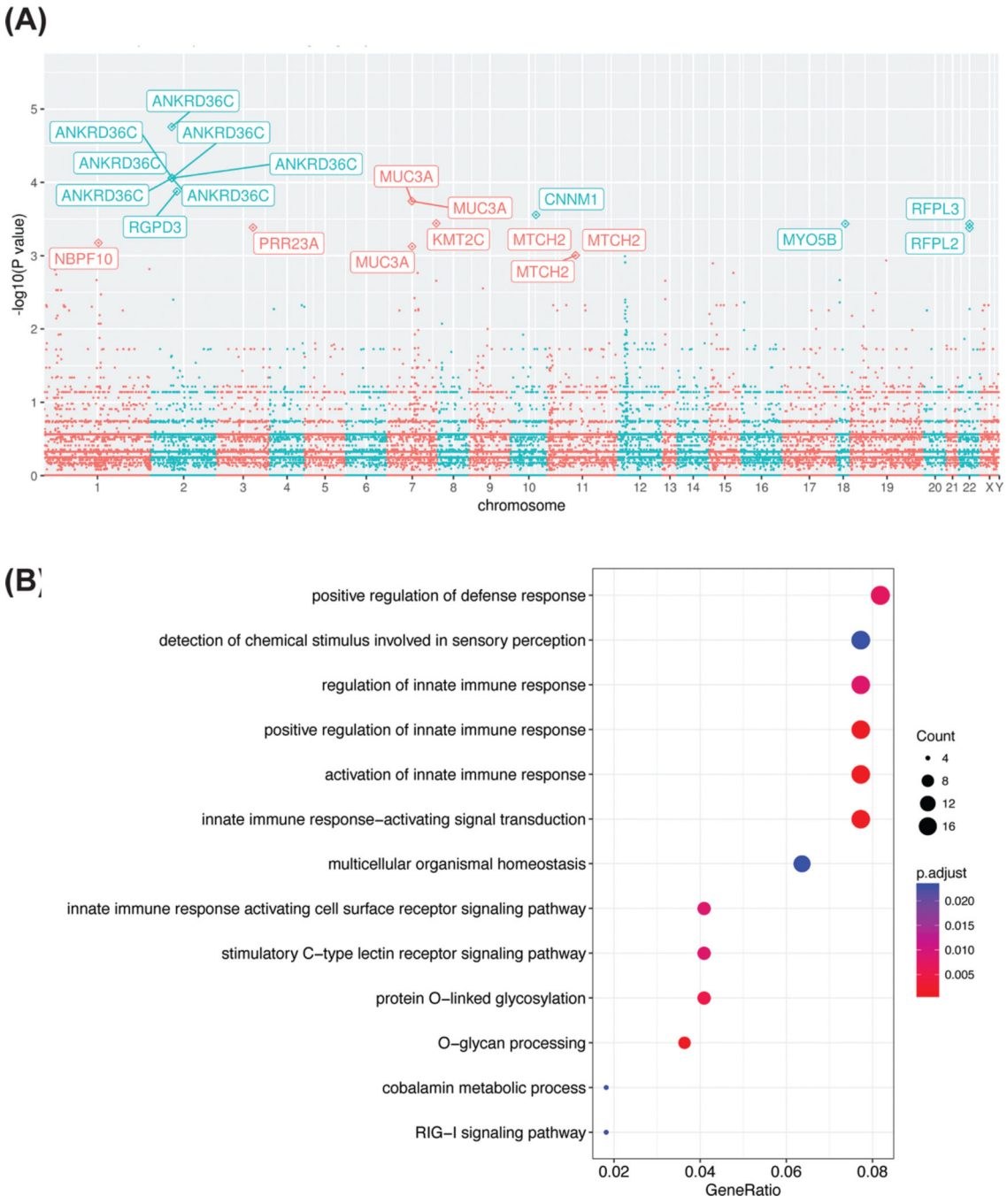

Fig. 2.

PLINK association test. (**A**) A Manhattan plot demonstrates the most significant variations identified in the association test. The *x*-axis represents chromosomes and the *y*-axis indicates the log converted *p*-values of the association results. Highly significant variations are labeled. Note, the highly significant *ANKRD36C* variants. (**B**) Pathways associated with iTTP. For this, all the significant SNVs associated with iTTP from the PLINK output were mapped onto their corresponding genes. These genes were then used to search for enrichment in gene ontology biological processes using the R-package clusterProfiler.[29]

Only the topmost significantly enriched pathways are shown. The *x*-axis represents the enrichment score. The size of each point represents the number of genes associated with the corresponding pathway. The color represents the *p*-value. iTTP, immune-mediated thrombotic thrombocytopenic purpura; SNV, single nucleotide variant.

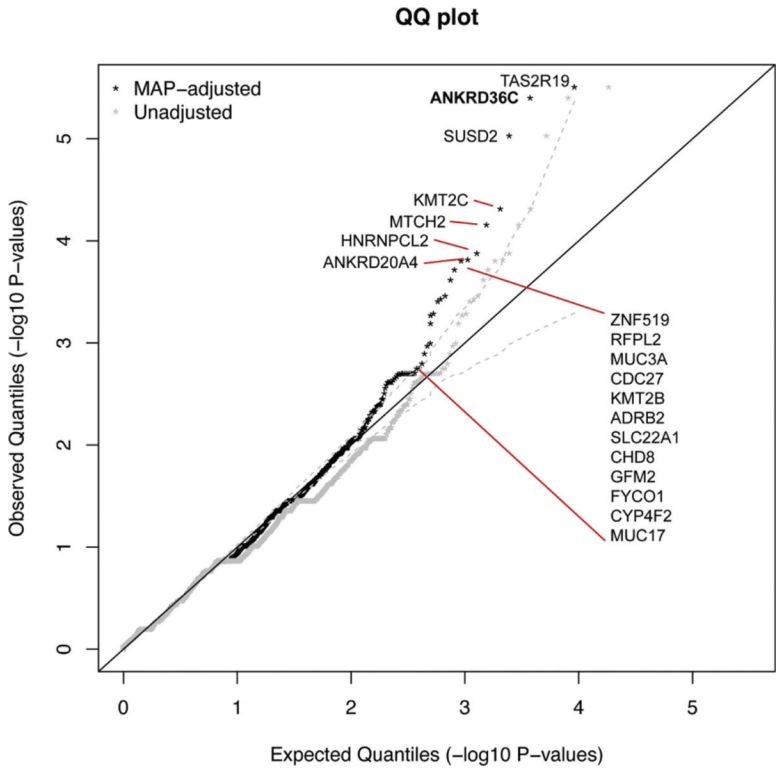

Fig. 3.

Quantile–quantile (Q–Q) plot demonstrating the most affected genes in iTTP. The analysis was done using R-package SKAT.[57] The expected *p*-values of genes on the *x*-axis were plotted against the observed *p*-values on the *y*-axis. Unadjusted and minimum achievable *p*-values (MAP) are shown in *gray* and *black*, respectively. Top significant genes based on MAP values are labeled. For descriptions of all the genes, please see ►Supplementary Table S3. iTTP, immune-mediated thrombotic thrombocytopenic purpura.

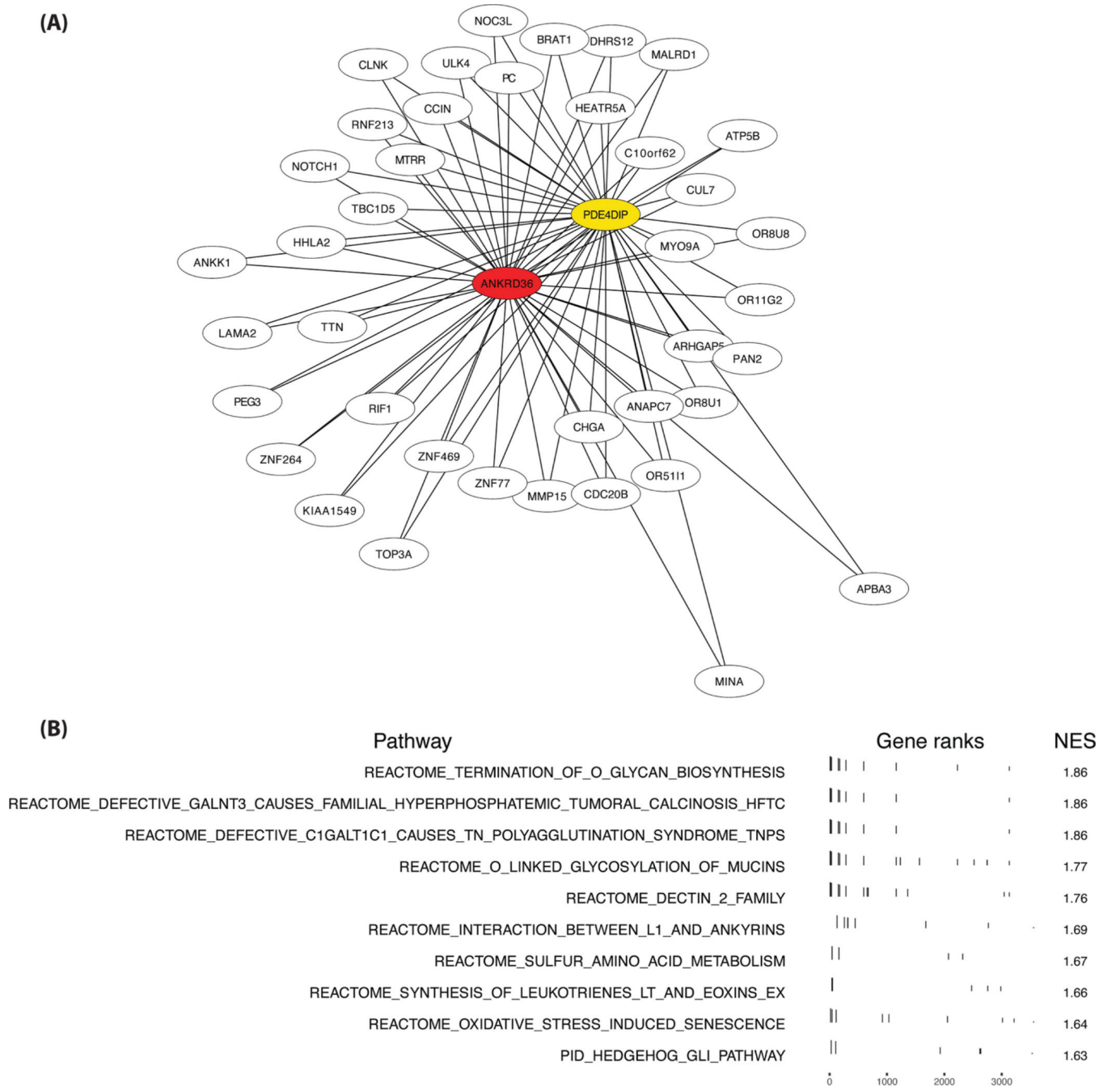

Fig. 4.

Epistatic network analysis. (**A**) Subnetwork shows the top two hub genes, ankyrin repeat domain-containing protein (*ANKRD*)*36C* and phosphodiesterase (PDE)4D interacting protein PDE4DIP in the epistatic network. The pairwise epistatic relationship between genes was calculated using PLINK and the *p*-values of the analysis were used as weights to construct an undirected network with nodes being the genes and the edges represent epistatic relationships between gene pairs. The edge weights were determined by the *p*-values. The hub genes in this network were identified using the cytoHubba[26] app in Cytoscape.[25] (**B**)

Top pathways affected by the hub genes in the epistatic network are shown. Gene set enrichment analyses were performed on gene list sorted based on centrality measure edge percolated component (EPC). The analysis was performed using R-package FGSEA[30] with the REACTOME database.[32] Only the top pathways sorted by the normalized enrichment score (NES) are shown.

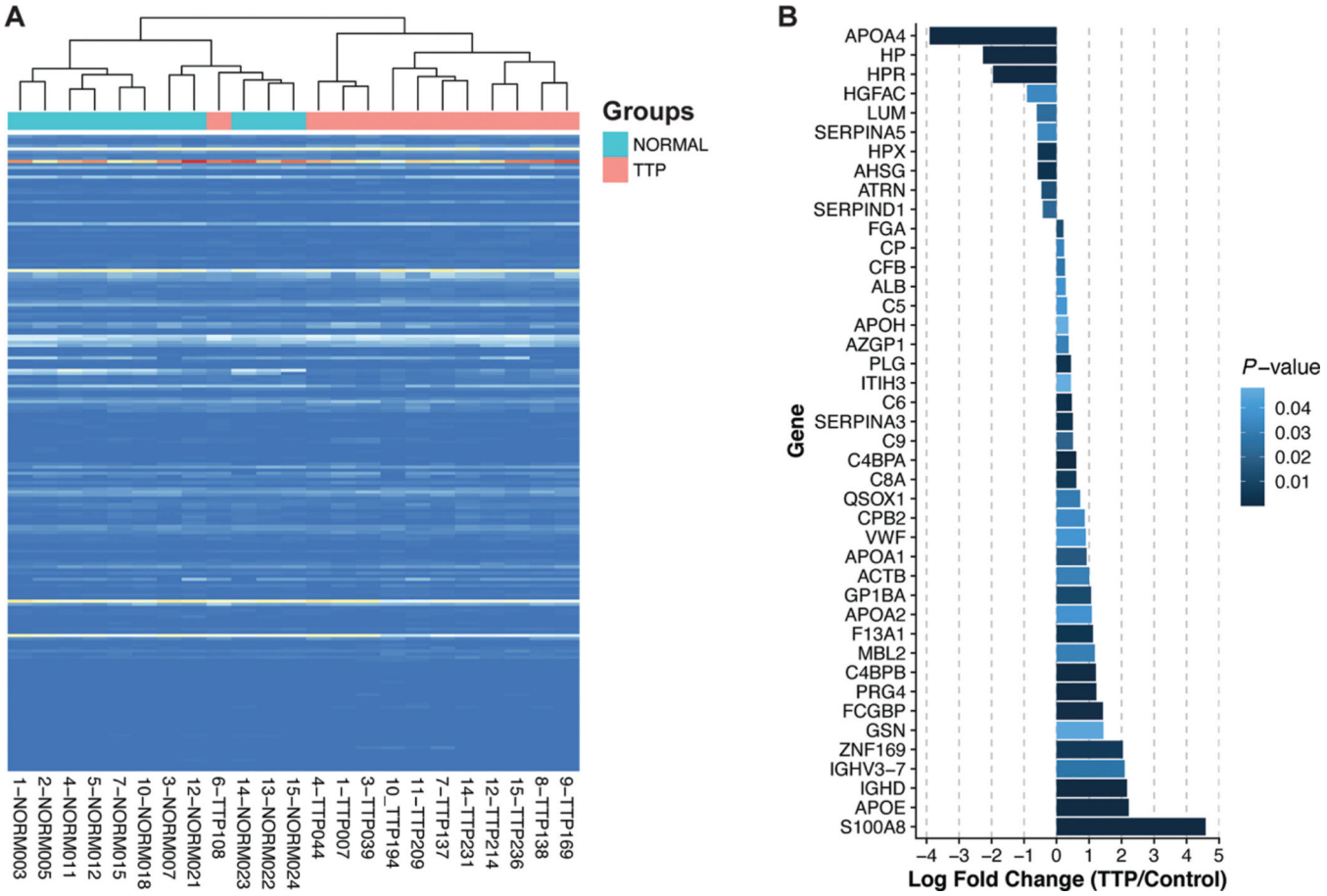

Fig. 5.

Glycoprotein profiles in cases and controls. (**A**) Heatmap shows the clustering of iTTP and control samples using the normalized counts for glycoproteins estimated using mass spectrometry. The clustering was done after removing the outliers. For the full dataset, please see ►Supplementary Fig. S4. (**B**) Differential abundance of glycoproteins in iTTP versus controls is shown. The x-axis shows the log2-fold change (LFC) and the y-axis shows the genes sorted based on LFC. The bars are colored based on p-values as shown in the legend. iTTP, immune-mediated thrombotic thrombocytopenic purpura.

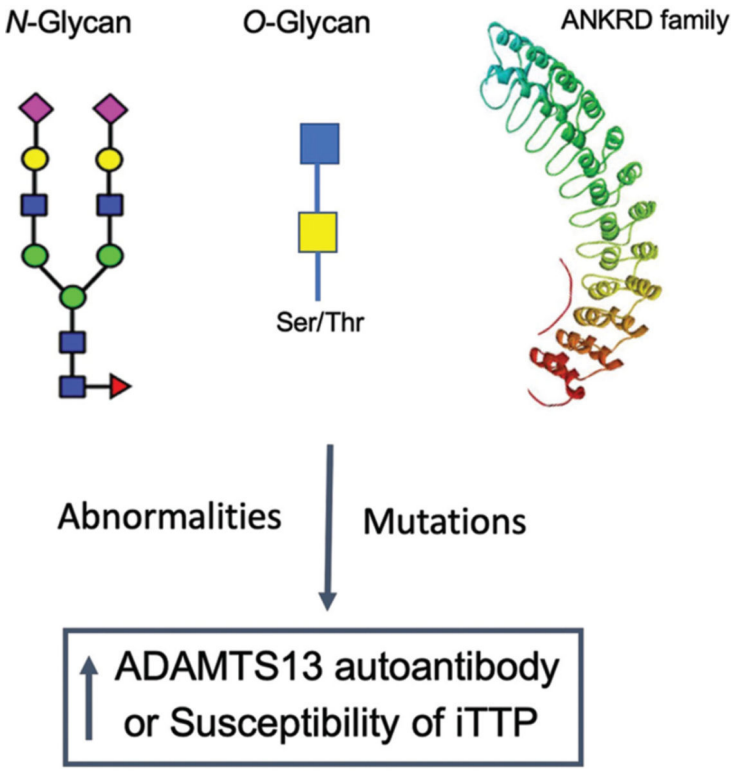

Fig. 6.

A presumptive hypothesis underlying how abnormalities in glycosylation and ANKRD gene family may lead to immune-mediated thrombotic thrombocytopenic purpura (iTTP).

Table 1

Demographic and clinical information of 40 patients with iTTP

Category	Values
Demographic	
Number of patients	40
Age, median (IQR)	44 (35–54)
Male, *n* (%)	14(35)
Female, *n* (%)	26 (65%)
Race	
Black, *n* (%)	30 (75)
White, *n* (%)	10(25)
Total episodes, median (IQR)	1.3 (1.1 –1.6)
Initial presentation	
Central nerve system signs/symptoms, *n* (%)	22 (55)
Abdominal pain, *n* (%)	11 (27.5)
Chest pain, *n* (%)	2(5)
Bleeding, *n* (%)	8(20)
Comorbidity	
Hypertension, *n* (%)	17 (42.5)
Diabetes mellitus, *n* (%)	9(22.5)
Obesity, *n* (%)	10(25)
Systemic lupus erythematosus, *n* (%)	4(10)
Human immunodeficiency viruses, *n* (%)	4(10)
Laboratory	
Platelet count ($x10^9$/L), median (IQR)	13 (11–24)
Hematocrit (%), median (IQR)	24 (22–29)
Lactate dehydrogenase (U/L), median (IQR)	839 (540–1505)
Creatine (mg/dL), median (IQR)	1.2 (0.9–1.8)
Haptoglobin (mg/dL), median	<30
Prothrombin (s), median (IQR)	15.8 (14.1–15.7)
aPTT (s), median (IQR)	30 (27–33)
D-dimer (ng/mL), median (IQR)	2,435 (1,177–6,421)
Troponin-I (ng/mL), median (IQR)	0.41 (0.04–2.30)
ADAMTS13 activity (U/dL), median	<5%[a]
Inhibitor (U/mL), median (IQR)	1.1 (0.4–1.9)[a]
Therapy	
Number of TPE, median (IQR)	15 (9–24)
Corticosteroids, *n* (%)	37 (92.5)
Vincristine, *n* (%)	6(15)

Category	Values
Cyclophosphamide, *n* (%)	2(5)
Rituximab, *n* (%)	22 (55)
Bortezomib	2(5)
Splenectomy, *n* (%)	3(7.5)
Outcome	
Single remission., *n* (%)	16 (40)
Exacerbation/relapse/remission, *n* (%)	24 (60)
Death, *n* (%)	3(7.5)
Length of stay in hospital (d), median (IQR)	19 (13–38)
Follow-up days, median (IQR)	407 (98–1,822)

Abbreviations: aPTT, activated thromboplastin time; IQR, interquartile range; LOS, length of stay; *n*, number of subjects; TPE, therapeutic plasma exchange.

[a]At the initial diagnosis.

Table 2

NonsynonymousmutationsinANKRD36C

CHR	Position	dbSNP ID	Ref	Alt	Exon	Ref AA	Alt AA	Protein position	CADD score	Allele freq. TTP	Allele freq. normal
2	96593000	rs1 11976783	A	G	exon28	I	T	634	2.321	0.375	0
2	96592982	-	T	C	exon28	E	G	640	1.606	0.325	0
2	96617111	rs76474100	G	A	exon15	R	X	417	27.2	0.325	0
2	96617113	rs80297803	G	A	exon15	P	L	416	16.49	0.325	0
2	96617125	rs75585230	T	C	exon15	K	R	412	0.002	0.325	0
2	96617132	rs75695780	T	C	exon15	K	E	410	0.381	0.325	0
2	96617155	rs76752473	A	G	exon15	I	T	402	0.012	0.325	0
2	96593016	rs79307257	C	A	exon28	D	Y	629	5.294	0.4125	0.1667
2	96593025	rs75189823	C	T	exon28	D	N	626	3.154	0.4125	0.1667
2	96521154	rs2951081	C	G	exon84	D	H	1985	12.3	0.4	0.1667

Abbreviations: AA, amino acid; CADD, Combined Annotation Dependent Depletion; CHR, Chromosome; dbSNP, Single Nucleotide Polymorphism Database; TTP, thrombotic thrombocytopenic purpura.